IEEE Access
Multidisciplinary | Rapid Review | Open Access Journal

Received January 8, 2019, accepted January 21, 2019, date of publication February 14, 2019, date of current version February 27, 2019.

Digital Object Identifier 10.1109/ACCESS.2019.2895154

Timely Two-Way Data Exchanging in Unilaterally Powered Fog Computing Systems

YUNQUAN DONG[1], (Member, IEEE), ZHENGCHUAN CHEN[2], (Member, IEEE), AND PINGYI FAN[3,4], (Senior Member, IEEE)

[1]School of Electronic and Information Engineering, Nanjing University of Information Science and Technology, Nanjing 210044, China
[2]School of Microelectronics and Communication Engineering, Chongqing University, Chongqing 400044, China
[3]Department of Electrical Engineering, Tsinghua University, Beijing 100084, China
[4]Tsinghua National Laboratory for Information Science and Technology, Tsinghua University, Beijing 100084, China

Corresponding author: Zhengchuan Chen (czc@cqu.edu.cn)

This work was supported in part by the National Natural Science Foundation of China under Grant 61701247 and Grant 61771283, in part by the Jiangsu Provincial Natural Science Research Project under Grant 17KJB510035, in part by the project funded by the Priority Academic Program Development of Jiangsu Higher Education Institutions, in part by the Startup Foundation for Introducing Talent of Nanjing University of Information Science and Technology under Grant 2243141701008, in part by the National Key Research and Development Program of China under Grant 2016YFE0121100, and in part by the Program for Innovation Team Building at colleges and universities in Chongqing, China, under Grant CXTDX201601006.

ABSTRACT Fog computing is attracting more and more attention to the next-generation wireless communication systems. In this paper, we consider such a mobile edge scenario where a fog node and a mobile user exchange their data in a two-way manner and only the fog node has a constant power supply. In particular, the fog node performs energy transfer when it is not transmitting information and the mobile user has an energy harvesting capability. For this scenario, we investigate the timeliness of the two-way data exchange between the fog node and the mobile user in terms of age of information (AoI) and derive closed-form average AoI for both directions, as well as the achievable data rate of the mobile user. We also discuss the achievable tradeoff on the average downlink/uplink AoIs and the achievable tradeoff on downlink/uplink data rates, which explicitly present the performance limit of the system in terms of timeliness and efficiency.

INDEX TERMS Age of information, two-way data exchange, fog computing.

I. INTRODUCTION

The Internet of things (IoT) is linking more and more smart devices (e.g., mobile phones, tablets, TVs, wearable devices, wireless sensors, connected vehicles) to the Internet. It is predicted that by 2020, the amount of active smart devices would be as high as 50 billion, with an average of 6.58 for each person [1]. Also, the network traffic will be increasing at an annual-growing-rate around 53% [2]. The computational capability of smart devices, however, is generally limited and insufficient to handle the increasing data traffic. Therefore, mobile cloud computing (MCC) has been proposed to move computational intensive functions to the cloud, i.e., a set of powerful servers [3], [4]. Through centralized management of available resources, MCC can provide smart devices with powerful and flexible computations. Since the cloud is usually located far from mobile users, however, the data exchange in MCC systems often suffers from large latency [5]. To address this issue, mobile edge computing (MEC) was proposed to move cloud servers to the edge of communication networks (e.g., integrated into base stations) so that the servers can be close to mobile users [6]. Fog computing (FC) is one of the most promising kind of MEC which can provide closer computations for mobile users [7], [8]. By connecting and exploring various devices (e.g., small BSs, WIFI APs, vehicles, collectively referred to as *fog nodes*) with strong computational capability, FC systems can serve mobile users over large areas in a distributed manner, and thus is especially suitable for IoT applications.

In addition to the limitation in computational capability, smart devices are also energy limited in general. Due to device size constraints and cost considerations, the battery capacity of a smart device is generally small, which is insufficient to support many mobile applications. Among solutions to this problem, radio frequency based wireless power transfer (WPT) is the most promising one, which can charge remote smart devices wirelessly [9]. In fact, current commercial WPT transmitters can efficiently deliver tens of microwatts power to smart devices over a distance of more than 10 meters, and thus is adequate for many low-power devices [10].

Therefore, the research on FC and MEC systems powered by WPT are gaining more and more attentions [9], [11]–[14]. In particular, the performance of these systems are often measured by the computation rate which quantifies the number of computation bits over each block and the offloading delay which is defined as the latency in offloading data to fog nodes (or mobile users) [9], [11]. For example, for a multi-user MEC network powered by WPT, the sum computation rate over all users are maximized in [11]. In [12], the weighted-sum computation rate of all users was maximized through optimal beamforming in a similar system with a multi-antenna access point (AP). Computation rate can also be maximized by minimizing network energy consumption [12] or maximizing network energy efficiency [13], which can be achieved by scheduling transmit power and time resources at APs and mobile users. Moreover, Mao *et al.* [14] investigated the tradoff between energy efficiency and offloading delay in a multi-user WPT powered MEC system.

Since the prevalence of IoT has spawned a plethora of real-time services that require timely information/status updates in MEC systems, efficient characterization of the computations freshness becomes a matter of urgency. Unfortunately, neither the computation rate nor the offloading delay is adequate to specify the freshness of the received data, especially when the intensity of energy transfer is weak. Note that when delay is small, the received data could not be fresh if the computation rate is low and the currently available data was generated a long time ago; when the computation rate is high, the received data would not be fresh either since the data would suffer from large queueing delays. To convey the freshness of the received information, therefore, a new metric was proposed in [15], i.e., *age of information* (AoI).

AoI is defined as the elapsed time since the generation of the latest received data [15]. Thus, AoI exactly reflects the freshness of the newest available data at the receiver. Since AoI is closely related to queueing theory, it has been studied in various queueing systems, e.g., *M/M/1, M/D/1* and *D/M/1* systems [15], and under several serving disciplines, e.g., first-come-first-served (FCFS) [15], last-generate-first-served (LGFS) [16]. The zero-wait policy where a new data packet would be served immediately after the completion of previous packet was also investigated in [17]. The serving disciplines mentioned above may find their respective applications in various scenarios. However, none of them can be generally optimal. Thus, many works were motivated to design packet scheduling schemes. For example, the benefit of dropping any arriving data packets seeing one or more waiting packets was discussed in [18]. The method of replacing the head-of-line packet with the latest arriving packet was studied in [19].

In this paper, we shall investigate the fundamental limits of timeliness and efficiency in a two-way data exchanging FC system as shown in Fig. 1. In particular, only the fog node has a constant energy supply. When the fog node is not transmitting data, it transfers energy to the mobile user using wireless power transfer. By harvesting and using the transferred energy, the mobile user transmits its data packets to the fog node according to the best-effort policy, i.e., performing a block of transmission as soon as it has collected enough energy to do so. This model is especially relevant to biomedical communications where a sensor is implanted inside human body and needs to timely communicate with a remote monitor through a fog node [20], [21]. For safety and implementability concerns, the sensor does not have a battery. To provide necessary control and energy for the sensor, a joint information-energy transmitter (i.e., a fog node) is placed in the room where the patient spends most of his time. Using the transferred energy, the senor can then report the health status of the patient to the monitor.

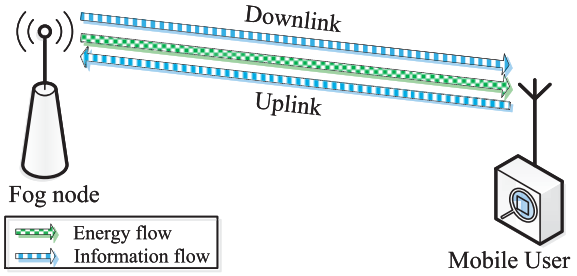

FIGURE 1. Two-way data exchanging FC system.

The uplink (from the mobile user to the fog node) AoI of the two-way data exchanging FC system has been investigated in the low signal-to-noise ratio (SNR) regime in [22]. In this paper, we shall jointly consider the average AoI in both directions as an extension. To be specific, we investigate the data exchanging capability of the system under the unique energy supply constraint in terms of average downlink AoI, average uplink AoI, downlink data rate, and uplink data rate. These results present a full characterization of the achievable timeliness and the achievable efficiency of the system in the low SNR regime. The main contributions of the paper are summarized as follows:

- We present average downlink AoI $\overline{\Delta}_{\mathrm{D}}$ as a function of downlink data rate p in closed form. We show that when p either goes to zero or approaches the maximal downlink data rate $p_{\max}$ (the maximal p ensuring a stable queue), the average downlink AoI goes to infinity. Thus, it is beneficial to control downlink data rate and spare some energy for uplink data transmissions.
- We present average uplink AoI $\overline{\Delta}_{\mathrm{U}}$ under the best-effort policy as a function of downlink data rate p in closed form. We show that the average uplink AoI converges to some constant as p goes to zero and goes to infinity as p approaches $p_{\max}$. Together with the result on average downlink AoI, we can also determine the achievable region of average downlink/uplink AoI pairs $(\overline{\Delta}_{\mathrm{D}}, \overline{\Delta}_{\mathrm{U}})$, which specifies the achievable tradeoff of the system in terms of timeliness.
- We also present uplink data rate q under the best-effort policy as a function of downlink data rate p in closed form. In particular, as p goes to zero, uplink data rate q is a constant; as p approaches $p_{\max}$, the uplink data rate

TABLE 1. Notations (DL=downlink, UL=uplink).

P_{t}	transmit power of fog node	$S_{\mathrm{D}k}$	service time of a packet
T_{B}	block length (unit: second)	A_k	no. of packets arrived during S_k
$\mathtt{W}$	system bandwidth	X_k	DL inter-arrival time
$\mathtt{N}_0$	noise spectrum density	$T_{\mathrm{D}k}$	DL system time
α	pathloss exponent	$W_{\mathrm{D}k}$	DL waiting time
β	βP_{t} is the transmit power of mobile user	$S_{\mathrm{Tx}k}$	no. of transmissions to deliver a UL packet
η	energy transfer efficiency	$S_{\mathrm{U}k}$	no. of blocks to deliver a UL packet
d	distance between fog node and mobile user	$T_{\mathrm{U}k}$	UL system time
ℓ	no. of nats per packet	$B_{\mathrm{D}l}$	DL busy period
p	DL data rate (prob. generating a packet each block)	$I_{\mathrm{D}l}$	DL idle period
q	UL data rate	$U_{\mathrm{D}}(n)$	generation time of the newest DL packet
γ_n	power gain of block n	$U_{\mathrm{U}}(n)$	generation time of the newest UL packet
b_n	no. of nats can be delivered in block n	$\Delta_{\mathrm{D}}(n)$	DL AoI at block n
E_n	harvested energy in block n	$\Delta_{\mathrm{U}}(n)$	UL AoI at block n
e_j	harvested energy within j DL idle blocks	$\bar{\Delta}_{\mathrm{D}}$	average DL AoI over infinite time
e_{r}	remaining energy of mobile user	$\bar{\Delta}_{\mathrm{U}}$	average UL AoI over infinite time
τ_{H}	no. of DL idle blocks to accumulate $P_{\mathrm{t}}T_{\mathrm{B}}$ of energy	$\boldsymbol{\pi}$	stationary distribution of queue length
n_k	arrival epoch of packet k	$L_{\mathrm{a}}^{+}(n)$	queue length at arbitrary epochs n
n'_k	departure epoch of packet k	$L_{\mathrm{d}}^{+}(k)$	queue length at the departure of packet k
p_j^{s}	prob. of DL service time $S_{\mathrm{D}k}$ being j blocks	N	no. of blocks under consideration
p_j^{a}	prob. of j packets arriving during $S_{\mathrm{D}k}$	K	no. of packets delivered over N blocks
θ	$\theta = \frac{\lambda \mathtt{N}_0 d^{\alpha} \ell}{P_{\mathrm{t}} T_{\mathrm{B}}}$	ρ	$\rho = \frac{\beta \lambda d^{\alpha}}{\eta}$

goes to zero. This result specifies the achievable region of data rate pairs (p, q), which is the best achievable efficiency of the system.

- We further investigate the average uplink AoI and the uplink data rate under the save-and-transmit policy in closed form. As shown in our numerical and Monte Carlo results, the best-effort policy yields the same data rate as the save-and-forward policy but has slightly larger average AoI. However, the best-effort is more practical to implement than the save-and-transmit policy, since the save-and-transmit policy requires large energy buffers and full-duplex transceivers.

The rest of the paper is organized as follows. Section II presents the system model and the AoI model. In Section III, we develop closed-form average downlink AoI and its asymptotic behaviors. In Section IV, we consider the average uplink AoI and the uplink data rate under the best-effort policy, as well as their asymptotic behaviors. The performance of the system under the save-and-transmit policy is also discussed in this section. Finally, numerical results are provided in Section V and our work is concluded in Section VI. Table 1 lists the notations used in this paper.

Notations: We use boldface letters to denote vectors and matrices, use $\tau = 1, \cdots, T$ to index time, use $k = 1, 2$ to index nodes, and use $\bar{k} = 3 - k$ to refer to the other node. $\mathbb{R}_{++}^n$ and $\mathbb{Z}_{++}^n$ denote the n-dimensional vector of positive real numbers and positive integers, respectively. In addition, $(\cdot)^{\mathrm{T}}$ denotes the transpose operation.

II. SYSTEM MODEL

We consider a two-way data exchanging FC system as shown in Fig. 1, where a fog node and a mobile user exchange their data (in packets) through block Rayleigh fading channels. The fog node has a constant power supply while the mobile user does not. In each block, the fog node generates a data packet with a certain probability. Afterwards, the generated packet will be delivered to the mobile user over the *downlink channel*. Since the fog node may take several blocks to complete the transmission of a packet, the fog node would often be busy transmitting data. In blocks when the data queue of the fog node is empty and no new packet is generated, the fog node will transmit energy to the mobile user though wireless power transfer. Upon receiving enough energy, the mobile user transmits its packet to the fog node via the *uplink channel*.

A. CHANNEL MODEL

On downlink and uplink channels, we consider the following assumptions.

A1 *Block Rayleigh-Fading:* Time is discrete and the period between epoch n and epoch $n + 1$ is referred to as block n. The channel power gain γ_n remains unchanged in each block and varies among blocks according to the exponential distribution

$$f_{\gamma}(x) = \lambda e^{-\lambda x}.$$

A2 *AWGN Noise:* Received signals suffer from additive white Gaussian noise (AWGN).

A3 *Low SNR Regime:* Received SNR is much smaller than unity due to limited transmit power and large transmit distance.

A4 *Time Division Duplex:* Downlink transmissions and uplink transmissions occur at different periods and use different frequency bands.

A5 *Channel Reciprocity:* The downlink channel and the uplink channel share the same channel model (including parameters). However, the corresponding instantaneous channel gains are independent from each other.

We denote the transmit power of the fog node as P_{t} for both information transmission and energy transfer. In the uplink,

the mobile node transmits information at power βP_{t}, where $0 < \beta < 1$ is a constant. Let T_{B} be the block length, $\mathtt{W}$ be the limited system bandwidth, and $\mathtt{N}_0$ be the noise spectrum density. We also denote the distance between the fog node and the mobile user as d and the pathloss exponent as α. The data (in nats) that can be transmitted to the mobile user in a block is given by

$$b_n = T_{\mathrm{B}}\mathtt{W}\log\left(1+\frac{\gamma_n P_{\mathrm{t}}}{\mathtt{W}\mathtt{N}_0 d^{\alpha}}\right) \approx \frac{\gamma_n P_{\mathrm{t}} T_{\mathrm{B}}}{\mathtt{N}_0 d^{\alpha}}, \tag{1}$$

where the approximation follows the *Low SNR* assumption. Thus, b_n also follows the exponential distribution. With slight confusion, we denote the waiting time of the k-th data packet as W_k and the number of blocks under consideration as N (see Subsection III-A and Subsection II-C, respectively).

B. DATA EXCHANGE MODEL

The following assumptions specify the data arriving (generating) model and the data serving (transmitting) model.

- U1 *Bernoulli Arrival at Fog Node:* In each block, the fog node generates a data packet of ℓ nats with probability p, which is referred to as *downlink data rate*.
- U2 *FCFS Policy at Fog Node:* The data packets generated at the fog node are put into a data queue and then served according to the FCFS discipline.
- U3 *Best-Effort Policy at Mobile User:* The mobile user performs a block of transmission with transmit power βP_{t} as soon as it has collected sufficient energy. In addition, the mobile user generates a data packet immediately after the completion of previous packet.
- U4 *Immediate Use of Energy:* Harvested energy can be used in the same block in which it is harvested.

We denote the number of blocks required to complete the transmission of a downlink data packet as *service time* S_{D}. According to [23], S_{D} follows Poisson distribution[1]

$$p_j^{\mathrm{s}} = \Pr\left\{\sum_{i=1}^{j-1} b_i < \ell, \sum_{i=1}^{j} b_i \geq \ell\right\} = \frac{\theta^{j-1}}{(j-1)!}e^{-\theta}, \tag{2}$$

where $j = 1, 2, \cdots$, and

$$\theta = \frac{\lambda \mathtt{N}_0 d^{\alpha}\ell}{P_{\mathrm{t}}T_{\mathrm{B}}}. \tag{3}$$

The probability generating function (PGF) and the first two order moments of S_{D} are, respectively, given by

$$G_{S_{\mathrm{D}}}(z) = \mathbb{E}\left(z^{S}\right) = ze^{\theta(z-1)}, \tag{4}$$

$$\mathbb{E}(S_{\mathrm{D}}) = \lim_{z\to 1^-} G'_{\mathrm{S}}(z) = 1+\theta, \tag{5}$$

$$\mathbb{E}(S_{\mathrm{D}}^2) = \lim_{z\to 1^-} G''_{\mathrm{S}}(z) + G'_{\mathrm{S}}(z) = \theta^2 + 3\theta + 1. \tag{6}$$

Note that equations (2) and (4)–(6) are derived based on the low SNR assumption A5. These results provide great convenience for our analysis on downlink and uplink AoIs which follows. For cases where assumption A5 does not hold, the probability distribution of service time S_{D} would be much more complex. Nevertheless, once the corresponding probability is obtained, the following analysis would be similar to that of this paper.

In each block when the data queue of the fog node is empty and no new data packet arrives, the fog node transfers energy to the mobile user. Let η be the energy transfer efficiency, the energy received by the mobile user would be

$$E_n = \eta\gamma_n d^{-\alpha} P_{\mathrm{t}} T_{\mathrm{B}}. \tag{7}$$

Upon receiving enough energy (the remaining energy is larger than $P_{\mathrm{t}}T_{\mathrm{B}}$), the mobile user performs a block of transmission immediately. In blocks when the mobile user does not have sufficient energy, the mobile user remains silent.

C. AGE OF INFORMATION

In this section, we develop a framework of discrete age of information that is especially applicable to the data exchange over block fading channels.

Definition 1: In block n, downlink age of information is the difference between epoch n (the beginning of the block) and the generation epoch $U_{\mathrm{D}}(n)$ of the latest received data packet at the mobile user,

$$\Delta_{\mathrm{D}}(n) = n - U_{\mathrm{D}}(n).$$

Likewise, uplink age of information is defined as $\Delta_{\mathrm{U}}(n) = n - U_{\mathrm{U}}(n)$.

Remark 1: In our model, AoI does not change within each block, which is different from the continuous AoI model in [15] and is a more suitable for discrete-time communication systems.

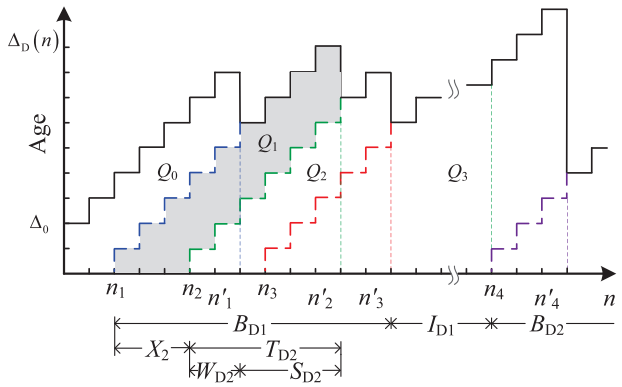

FIGURE 2. Sample path of downlink AoI $\Delta_{\mathrm{D}}(n)$ (the upper envelope in bold). For the k-th packet, $X_k = n_{k+1} - n_k$ is the inter-arrival time, $W_{\mathrm{D}k}$ is the waiting time, $S_{\mathrm{D}k}$ is the service time, and $T_{\mathrm{D}k} = W_{\mathrm{D}k} + S_{\mathrm{D}k}$ is the system time. $B_{\mathrm{D}l}$ and $I_{\mathrm{D}l}$ refer to the l-th downlink busy period and idle period, respectively.

Fig. 2 presents a sample variation of downlink AoI $\Delta_{\mathrm{D}}(n)$ with initial age Δ_0. Data packets are generated at arrival epochs $\{n_k, k = 1, 2, \cdots\}$ and are completely transmitted at departure epochs n'_k. The *inter-arrival time* between neighboring packets is $X_k = n_k - n_{k-1}$ and the *downlink system*

[1] In our case, we have $j \geq 1$, which is slightly different from Poisson distribution. In addition, we say the service time is $S_k = 1$ even if its completion time is less than T_{B}.

time that packet k stays in the system is $T_{\mathrm{D}k} = n'_k - n_k$. Note that downlink system time is the sum of *waiting time* $W_{\mathrm{D}k}$ and service time $S_{\mathrm{D}k}$, i.e., $T_{\mathrm{D}k} = W_{\mathrm{D}k} + S_{\mathrm{D}k}$. A *downlink idle period* I_{D} is a period when the data queue of the fog node is empty and no new packet arrives. Thus, the energy transfer from the fog node to the mobile user occurs during downlink idle periods. Moreover, a *downlink busy period* B_{D} is a period when the fog node is busy transmitting data packets. Specifically, B_{D} is composed of 1) the service time (e.g., $S_{\mathrm{D}k}$) of an immediate packet following the previous idle period (or a busy period in case that the length of previous idle period is zero); 2) the downlink busy period generated by each of the packets (e.g., $i = 1, 2, \cdots, i_0$) arriving during the service time $S_{\mathrm{D}k}$ of this immediate packet.

It is observed that AoI increases linearly in time and is reset to the age of the newest received packet at the end of departure blocks. Over a period of N blocks where K downlink data packets are delivered, the average downlink AoI is defined as

$$\overline{\Delta}_{\mathrm{D}} = \lim_{N\to\infty} \frac{1}{N} \sum_{n=1}^{N} \Delta_{\mathrm{D}}(n).$$

Starting from the first block, the area under $\Delta_{\mathrm{D}}(n)$ can be seen as the concatenation of areas $Q_0, Q_1, \cdots$, and the triangular-like area of width T_K. Thus, we can express $\overline{\Delta}_{\mathrm{D}}$ as

$$\overline{\Delta}_{\mathrm{D}} = \lim_{N\to\infty} \frac{1}{N} \Big(Q_0 + \sum_{k=1}^{K-1} Q_k + \frac{1}{2} T_{\mathrm{D}K}(T_{\mathrm{D}K} + 1) \Big). \quad (8)$$

In the uplink, the mobile user adopts the best-effort policy. We denote the *uplink system time* of data packet k as $T_{\mathrm{U}k}$. Note that when downlink power transfer is weak, an uplink packet takes a long period to complete, which may cover several downlink idle periods and busy periods. Thus, $T_{\mathrm{U}k}$ includes the service time of the packet, the time for harvesting energy, and the time waiting for downlink power transfer (if any).

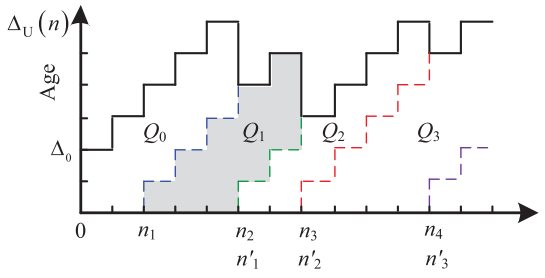

FIGURE 3. Sample path of uplink AoI $\Delta_{\mathrm{U}}(n)$ (the upper envelope in bold).

Consider a period of N blocks in which K (not necessarily equal is to the downlink case) data packets are transmitted to the fog node, as shown in Fig. 3. Similar to the downlink analysis, we have

$$\overline{\Delta}_{\mathrm{U}} = \lim_{N\to\infty} \frac{1}{N} \Big(Q_0 + \sum_{k=1}^{K-1} Q_k + \frac{1}{2} T_{\mathrm{U}K}(T_{\mathrm{U}K} + 1) \Big). \quad (9)$$

Given a downlink data rate p, we denote the achievable uplink data rate as $q(p)$, which is given by

$$q(p) = \lim_{N\to\infty} \frac{K}{N}. \quad (10)$$

III. DOWNLINK AGE OF INFORMATION

In this section, the average downlink AoI is derived in closed form. To do this, we first present the queueing model of the two-way data exchanging FC system. Next, we investigate the statistical characteristics of the queue and then solve for the average downlink AoI.

A. QUEUEING MODEL OF DOWNLINK TRANSMISSIONS

At the fog node, data packets are generated according to Bernoulli distribution (cf. *Assumption* U1) and are delivered with Poisson distributed service time (cf. (2)). Thus, the data queue can be modeled as a *Geom/GI/1* queueing system. For this system, we further assume late arrival protocol with delayed access. To be specific, data packets arrive at the end of blocks (e.g., n_k^-) and leave at the beginning of blocks (e.g., $n_k'^+$). Also, the service of data packets starts from the beginning of blocks and last for at least one block. We denote $L_{\mathrm{a}}^+(n)$ as the length (number of packets) of the data queue at the beginning of block n, in which the packet arriving at epoch n is counted and the packet leaves at epoch n is not. We refer to $L_{\mathrm{a}}^+(n)$ as *queue length at arbitrary epochs*.

Moreover, in the block during which the transmission of packet k is completed, we refer to the corresponding queue length $L_{\mathrm{d}}^+(k)$ as the *queue length at departure epochs*, i.e., $L_{\mathrm{d}}^+(k) = L_{\mathrm{a}}^+(n'_k)$. Since departure epochs must see an empty queue or the beginning of the service of a new data packet, these departure epochs are aftereffectless points of the queueing process. Denote the number of data packets arriving during service time S_{k+1} as A_{k+1}, the queue length at the departure of packet $k+1$ would be

$$L_{\mathrm{d}}^+(k+1) = \begin{cases} L_{\mathrm{d}}^+(k) - 1 + A_{k+1}, & L_{\mathrm{d}}^+(k) \geq 1, \\ A_{k+1}, & L_{\mathrm{d}}^+(k) = 0. \end{cases}$$

It is clear that $\{L_{\mathrm{d}}^+(k), k \geq 0\}$ is a Markov chain.

We denote the probability that j data packets arrive during the service time of a certain packet as $p_j^{\mathrm{a}} = \Pr\{A_k = j\}$, where $j = 0, 1, \cdots$. Hence, the probability transfer matrix $P = (p_{i,j})$ of $\{L_{\mathrm{d}}^+(k), k \geq 0\}$ would be

$$P = \begin{bmatrix} p_0^{\mathrm{a}} & p_1^{\mathrm{a}} & p_2^{\mathrm{a}} & p_3^{\mathrm{a}} & \cdots \\ p_0^{\mathrm{a}} & p_1^{\mathrm{a}} & p_2^{\mathrm{a}} & p_3^{\mathrm{a}} & \cdots \\ 0 & p_0^{\mathrm{a}} & p_1^{\mathrm{a}} & p_2^{\mathrm{a}} & \cdots \\ 0 & 0 & p_0^{\mathrm{a}} & p_1^{\mathrm{a}} & \cdots \\ \vdots & \vdots & \vdots & \vdots & \ddots \end{bmatrix}$$

In particular, we have the following proposition on A_k.

Proposition 1: The probability distribution and PGF of A are, respectively, given by

$$p_j^{\mathrm{a}} = (1-p)e^{-\theta p}\frac{(\theta p)^j}{j!} + pe^{-\theta p}\frac{(\theta p)^{(j-1)}}{(j-1)!}, \quad (11)$$

$$G_{\mathrm{A}}(z) = (1-p+pz)e^{\theta p(z-1)}. \quad (12)$$

Proof: See Appendix A. □

Following Foster's Theorem [24], one can prove that Markov chain $\{L_{\mathrm{d}}^+(k), k \geq 0\}$ is positive recurrence and the data queue at the fog node is stable only if the following *queueing constraint* is satisfied

$$p(\theta+1) < 1.$$

To be specific, one can find a set of Lyapunov functions $V(i)$ such that $\sum_i V(i)p_{i,j} = V(j)$ and $\sum_i V(i) < \infty$ when this constraint is satisfied. By normalizing $V(i)$, it is clear that Markov chain $\{L_{\mathrm{d}}^+(k), k \geq 0\}$ has a stationary distribution $\boldsymbol{\pi} = (\pi_0, \pi_1, \cdots)$ with $\pi_j = \lim_{k\to\infty} \Pr\{L_{\mathrm{d}}^+(k) = j\}$. Denote $G_{L_{\mathrm{d}}^+}(z) = \mathbb{E}(z^{L_{\mathrm{d}}^+})$ as the PGF of stationary queue length at departure epochs, we have the following proposition.

Proposition 2: If $(\theta+1)p < 1$, the PGF of stationary queue length at departure epochs is

$$G_{L_{\mathrm{d}}^+}(z) = \frac{(1-p-\theta p)(1-p+pz)(1-z)}{1-p+pz-ze^{\theta p(1-z)}}. \quad (13)$$

Proof: The proof mainly employs stationary equation $\boldsymbol{\pi} = \boldsymbol{\pi}P$ and the PGF of A_k (cf. (12)), which is similar to the proof of [23, Th. 1]. □

Moreover, the following lemma specifies the relationship between the stationary distribution of queue length in departure epochs and that in arbitrary epochs [23].

Lemma 1: At the fog node, the stationary distributions of queue length in departure epochs and the stationary distribution of queue length in arbitrary epochs are the same.

Therefore, the queueing behavior at the fog node can be determined by $G_{L_{\mathrm{d}}^+}(z)$. Based on *Proposition* 2 and *Lemma* 1, the PGF of downlink system time T_{D} of data packets can thus be determined.

Proposition 3: The PGF of downlink system time of each data packet is given by

$$G_{T_{\mathrm{D}}}(z) = \frac{(1-p-\theta p)z(1-z)}{pz-(z-1+p)e^{\theta(1-z)}}. \quad (14)$$

Proof: See Appendix B. □

By employing the L'Hôpital's rule [25], the average downlink system time can be obtained as

$$\mathbb{E}(T_{\mathrm{D}}) = \lim_{z\to 1^-} G'_{T_{\mathrm{D}}}(z) = 1+\theta+\frac{2p\theta+\theta^2 p}{2(1-p-\theta p)}. \quad (15)$$

Note that the downlink system time can be expressed as $T_{\mathrm{D}} = W_{\mathrm{D}} + S_{\mathrm{D}}$. Thus, it is observed from (15) that the average waiting time is given by $\mathbb{E}(W_{\mathrm{D}}) = \mathbb{E}(T_{\mathrm{D}}) - \mathbb{E}(S_{\mathrm{D}}) = \frac{2p\theta+\theta^2 p}{2(1-p-\theta p)}$, where $\mathbb{E}(S_{\mathrm{D}}) = 1+\theta$ is given by (5). Since the area of each Q_k is closely related to downlink system time $T_{\mathrm{D}k}$ (cf. (8) and Fig. 2) of the k-th data packet, *Proposition* 3 and (15) are very useful in calculating average downlink AoI.

B. AVERAGE DOWNLINK AGE OF INFORMATION

Based on the queueing model shown in Subsection III-A, various statistics of $\{L_{\mathrm{a}}^+(k), k \geq 0\}$ can be obtained. Using the derived statistics of $\{L_{\mathrm{a}}^+(k), k \geq 0\}$, we can then obtain the average downlink AoI readily, as shown in the following theorem.

Theorem 1: If $(\theta+1)p < 1$, the average downlink age of information is given by

$$\overline{\Delta}_{\mathrm{D}} = \frac{1}{p}+1+\theta+\frac{(-2+4p+3\theta p)\theta}{2(1-p-\theta p)}+\frac{(1-p-\theta p)(e^{\theta p}-1)}{p}, \quad (16)$$

where $\theta = \frac{\lambda_{\mathrm{N}_0} d^\alpha \ell}{P_{\mathrm{t}} T_{\mathrm{B}}}$. Otherwise, $\overline{\Delta}_{\mathrm{D}}$ would be infinitely large.

Proof: See Appendix C. □

To better understand (16), we would like to mention that $\mathbb{E}(X) = \frac{1}{p}$ is the average inter-arrival time between adjacent data packets, $\mathbb{E}(S_{\mathrm{D}}) = 1+\theta$ is the average service time of data packets, and the last two terms show the effect of the queueing process. In addition, θ is the ratio between packet length ℓ and $\mathbb{E}(b)$, e.g., $\theta = \frac{\ell}{\mathbb{E}(b)}$, where $\mathbb{E}(b) = \frac{P_{\mathrm{t}} T_{\mathrm{B}}}{\lambda_{\mathrm{N}_0} d^\alpha}$ is the average amount of information that can be transmitted during a block (cf. (1)).

In the following, we investigate two extreme cases of the data exchanging system and have the following results.

Corollary 1: If $(\theta+1)p \approx o$, where o is an infinitesimal, the average downlink AoI is given by

$$\overline{\Delta}_{\mathrm{D}} = 1+\theta+(1+\theta)\cdot\frac{1}{o}. \quad (17)$$

Proof: The corollary can be readily proved by using approximation $p \approx \frac{0}{1+\theta}$ in (16). □

In the case $(\theta+1)p \approx o$, the downlink channel is lightly occupied by packet transmissions and inter-arrival time would be large. Thus, the received data packets at the mobile user is not fresh in most times.

Corollary 2: If $(\theta+1)p \approx 1-o$, where o is an infinitesimal, average downlink AoI is

$$\overline{\Delta}_{\mathrm{D}} = 2+\frac{\theta}{2}+\frac{\theta(2+\theta)}{2(1+\theta)}\cdot\frac{1}{o}. \quad (18)$$

Proof: The corollary can be readily proved by using approximations $1-p-\theta p = o$ and $p \approx \frac{1}{\theta+1}$ in (16). □

When $(\theta+1)p$ approaches unity, downlink channel would always be busy with transmitting data packets. Thus, the waiting time of data packets can be arbitrarily long. As observed from *Corollary* 2, the average downlink AoI goes to infinity linearly as o approaches zero.

IV. UPLINK AGE OF INFORMATION

Under the best-effort policy, the mobile user performs a block of transmission whenever it has harvested sufficient energy. In addition, the mobile user may take several blocks of transmissions to complete a packet and take more blocks to harvest the required energy. In this section, we first investigate the property of the energy harvesting process and uplink service time, and then derive the average uplink AoI and the uplink

data rate in closed form. The average uplink AoI and uplink data rate under the save-and-transmit policy will also be studied.

A. ENERGY HARVESTING PROCESS

In our model, the fog node transfers energy to the mobile user during downlink idle periods. Since the energy transfer efficiency is definitely smaller than unity, the mobile user often takes several downlink idle blocks to accumulate sufficient energy to perform a block of transmission. In a period of j downlink idle blocks, we denote the harvested energy as

$$e_j = \sum_{i=1}^{j} E_{m_i} = \eta d^{-\alpha} P_{\mathrm{t}} T_{\mathrm{B}} \sum_{i=1}^{j} \gamma_{m_i},$$

where m_i is the index of the i-th block of this period and γ_{m_i} is the exponentially distributed power gain. It is clear that e_j follows the Erlang distribution. That is,

$$f_{e_j}(x) = \Big(\frac{\lambda d^{\alpha}}{\eta P_{\mathrm{t}} T_{\mathrm{B}}}\Big)^{j} \frac{x^{j-1}}{(j-1)!} e^{-\frac{\lambda d^{\alpha}}{\eta P_{\mathrm{t}} T_{\mathrm{B}}} x}.$$

Let τ_{H} be the number of downlink idle blocks for the mobile user to accumulate sufficient energy to perform a block of transmission and e_r be the remaining energy after the previous transmission. We have $\Pr\{\tau_{\mathrm{H}} = 0\} = \Pr\{e_r > \beta P_{\mathrm{t}} T_{\mathrm{B}}\}$ and

$$\Pr\{\tau_{\mathrm{H}} = j\} = \Pr\{e_r + e_{j-1} < \beta P_{\mathrm{t}} T_{\mathrm{B}}, e_r + e_j \geq \beta P_{\mathrm{t}} T_{\mathrm{B}}\}$$

for $j = 1, 2, \cdots$, where $\beta P_{\mathrm{t}} T_{\mathrm{B}}$ is the transmit power of the mobile user. Thus, the actual time to perform a block of uplink transmission is $s = \max\{1, \tau_{\mathrm{H}}\}$.

Note that energy transfer efficiency η is small, and the transmit distance is large in general. In each block, therefore, the harvested energy is not enough to perform a block of transmission and τ_{H} would be larger than 1 almost surely. Suppose that E_m of energy was harvested by the mobile user in the last block of previous period τ_{H}. According to (7), E_m follows the exponential distribution. In this block, a part of E_m would be consumed and the remaining energy, which is denoted as e_r, can be used for the next transmission. Due to the memoryless property of exponential distribution, we know that e_r follows the same distribution as E_m. Thus, we have,

$$\begin{aligned}\Pr\{\tau_{\mathrm{H}} = j\} &= \Pr\{e_j < \beta P_{\mathrm{t}} T_{\mathrm{B}}, e_{j+1} \geq \beta P_{\mathrm{t}} T_{\mathrm{B}}\} \\ &= \int_0^{P_{\mathrm{t}} T_{\mathrm{B}}} f_{e_j}(x)\mathrm{d}x \int_{P_{\mathrm{t}} T_{\mathrm{B}} - x}^{\infty} f_{e_1}(y)\mathrm{d}y \\ &= \frac{\rho^j}{j!} e^{-\rho}, \end{aligned} \tag{19}$$

where ρ is defined as

$$\rho = \frac{\beta \lambda d^{\alpha}}{\eta}. \tag{20}$$

Remark 2: In Monte Carlo simulations, the channel conditional can occasionally be so good (i.e., $\gamma_n \gg 1$) that the transferred energy would be amplified. Nevertheless, the statement that the harvested energy in a block is not enough to perform a block of transmission is true in most cases, especially when the distance between the mobile user and the fog node is large.

Following a similar analysis on downlink service time, the PGF and the first two order moments of the required number S_{Tx} of transmissions to deliver an uplink packet are, respectively, given by

$$\begin{aligned} G_{S_{\mathrm{Tx}}}(z) &= z e^{\frac{\theta}{\beta}(z-1)}, \\ \mathbb{E}(S_{\mathrm{Tx}}) &= 1 + \frac{\theta}{\beta}, \\ \mathbb{E}(S_{\mathrm{Tx}}^2) &= \frac{\theta^2}{\beta^2} + \frac{3\theta}{\beta} + 1. \end{aligned}$$

We denote the *uplink service time* as S_{U}, which includes the actual number (i.e., S_{Tx}) of transmissions for delivering the packet, and the time required for harvesting and accumulating energy. Thus, we have

$$S_{\mathrm{U}} = \sum_{i=1}^{S_{\mathrm{Tx}}} s_i. \tag{21}$$

In particular, the moments of S_{U} are given by the following proposition.

Proposition 4: The first-two order moments of the uplink service time S_{U} are, respectively, given by

$$\mathbb{E}(S_{\mathrm{U}}) = \big(\rho + e^{-\rho}\big)\big(1 + \frac{\theta}{\beta}\big),$$

$$\mathbb{E}(S_{\mathrm{U}}^2) = \big(\rho + e^{-\rho}\big)^2\big(\frac{\theta^2}{\beta^2} + \frac{2\theta}{\beta}\big) + \big(\rho^2 + \rho + e^{-\rho}\big)\big(1 + \frac{\theta}{\beta}\big).$$

Proof: See Appendix D. □

B. UPLINK SYSTEM TIME

In the downlink transmission, several busy periods may appear consecutively. Specifically, this happens when a new downlink packet (which starts a new downlink busy period) is generated immediately after the end of previous downlink busy period. In this case, we say that the length of the downlink idle period between the two consecutive downlink busy periods is zero, i.e., $I_{\mathrm{D}} = 0$. We denote the number of downlink busy periods coming uninterruptedly as F. Based on the distribution of downlink idle period $\Pr\{I_{\mathrm{D}} = j\} = (1-p)^j p$ where $j = 0, 1, \cdots$, the distribution and the first two order moments of F can be obtained as follows.

$$p_j^{\mathrm{f}} = \Pr\{F = j\} = p^j(1-p), \quad j = 0, 1, 2, \cdots, \tag{22}$$

$$\mathbb{E}(F) = \frac{p}{1-p}, \tag{23}$$

$$\mathbb{E}(F^2) = \frac{p(1+p)}{(1-p)^2}. \tag{24}$$

Suppose that the mobile user takes $S_{\mathrm{U}k}$ blocks of transmission to deliver uplink packet k to the fog node. Since $S_{\mathrm{U}k}$ maybe longer than one downlink idle period, uplink service time $S_{\mathrm{U}k}$ is often partitioned into several parts. In particular, the end of every block of $S_{\mathrm{U}k}$ can be a dividing point, following which there may exist one or more downlink busy periods.

Moreover, there may also exist some downlink busy periods before S_{Uk}.

We denote the period between the generation and the completion of an uplink packet as *uplink system time* T_U. It is clear that T_U is composed of uplink service time S_U and several downlink busy periods, and can be expressed as

$$T_U = S_U + \sum_{i=1}^{S_U} \sum_{j=1}^{F_i} B_{Dj}. \tag{25}$$

The first two order moments of downlink busy period B_D are given by the following proposition.

Proposition 5: The first-order and second-order moments of downlink busy period are, respectively, given by

$$\mathbb{E}(B_D) = \frac{1+\theta}{1-p-\theta p}, \tag{26}$$

$$\mathbb{E}(B_D^2) = \frac{(1+\theta)^2(1-p^2-\theta p^2)+\theta}{(1-p-\theta p)^3}. \tag{27}$$

Proof: See Appendix E. □

Based on aforementioned analysis and *Proposition* 5, we have the following proposition on uplink system time T_U.

Proposition 6: The moments of uplink system time are given by

$$\begin{aligned}\mathbb{E}(T_U) &= \mathbb{E}(S_U)\big(1+\mathbb{E}(F)\mathbb{E}(B_D)\big),\\ \mathbb{E}\big(T_U^2\big) &= \mathbb{E}(S_U^2)\Big(1+\mathbb{E}(F)\mathbb{E}(B_D)\Big)^2 + \mathbb{E}(S_U)\\ &\quad\cdot\Big(\mathbb{E}(F)\mathbb{E}(B_D^2) + \big(\mathbb{E}(F^2)-\mathbb{E}(F)-\mathbb{E}^2(F)\big)\mathbb{E}^2(B_D)\Big).\end{aligned} \tag{28}$$

Proof: The proposition can readily be proved based on (25). □

Note that the moments of T_U can readily be calculated based on (23)–(27).

C. AVERAGE UPLINK AoI UNDER BEST-EFFORT POLICY

In this subsection, we investigate average uplink AoI and uplink data rate as functions of downlink data rate. The main result of this part is summarized in the following theorem.

Theorem 2: If $(\theta+1)p < 1$, the average uplink AoI is

$$\begin{aligned}\overline{\Delta}_U = &+\frac{p(1+\theta)^2-(2-p)p^3(1+\theta)^3+\theta p(1-p)}{2(1-p)(1-p-\theta p)^2(1-p+p^2+\theta p^2)}\\ &+\left(\frac{\rho^2+\rho+e^{-\rho}}{\rho+e^{-\rho}}+\frac{(\rho+e^{-\rho})(\frac{3\theta^2}{\beta^2}+\frac{6\theta}{\beta}+2)}{1+\frac{\theta}{\beta}}\right)\\ &\cdot\frac{1-p+p^2+\theta p^2}{2(1-p)(1-p-\theta p)}+\frac{1}{2},\end{aligned} \tag{29}$$

the achievable uplink data rate is given by

$$q(p) = \frac{(1-p)(1-p-\theta p)}{(\rho+e^{-\rho})(1+\frac{\theta}{\beta})(1-p+p^2+\theta p^2)}, \tag{30}$$

where $\theta = \frac{\lambda N_0 \ell}{P_t T_B}$ and $\rho = \frac{\beta\lambda d^\alpha}{\eta}$. Otherwise, $\overline{\Delta}_U$ would be infinitely large and $q(p)$ would be zero.

Proof: *Theorem* 2 follows directly from *Proposition* 5 and *Proposition* 6. For more details, please refer to Appendix F. □

To obtain more insights, we further focus on the following two extreme cases.

Corollary 3: If $(\theta+1)p \approx o$, where o is an infinitesimal, the average uplink AoI and the uplink data rate are given by

$$\begin{aligned}\overline{\Delta}_U &= \frac{1}{2}\left(\frac{\rho^2+\rho+e^{-\rho}}{\rho+e^{-\rho}}+\frac{(\rho+e^{-\rho})(\frac{3\theta^2}{\beta^2}+\frac{6\theta}{\beta}+2)}{1+\frac{\theta}{\beta}}+1\right),\\ q &= \frac{1}{(\rho+e^{-\rho})(1+\frac{\theta}{\beta})}.\end{aligned}$$

Proof: This corollary follows the approximations $p \approx \frac{o}{1+\theta}$ and equations (29), (30). □

The condition $(\theta+1)p \approx 0$ indicates that downlink channel is lightly occupied and thus much energy can be transferred to the mobile user. Under the best-effort policy, both uplink AoI and uplink data rate would be finite, as shown in *Corollary* 3. In this case, the key parameters include the expected service time $\mathbb{E}(S_{Tx}) = 1+\frac{\theta}{\beta}$, the expected channel power gain $\frac{1}{\lambda}$ and the energy transfer efficiency η.

Corollary 4: If $(\theta+1)p \approx 1-o$ where o is an infinitesimal, the average uplink AoI and the uplink data rate are, respectively, given by

$$\begin{aligned}\overline{\Delta}_U &= \left(\frac{\rho^2+\rho+e^{-\rho}}{\rho+e^{-\rho}}+\frac{(\rho+e^{-\rho})(\frac{3\theta^2}{\beta^2}+\frac{6\theta}{\beta}+2)}{1+\frac{\theta}{\beta}}\right)\frac{1+\theta}{2\theta}\frac{1}{o},\\ q &= \frac{\theta}{(1+\theta)^2(\rho+e^{-\rho})}\cdot o.\end{aligned}$$

Proof: In this case, we approximately have $p = \frac{1}{1+\theta}$ and $1-p-\theta p = o$. The corollary can be readily proved by using the approximation in equations (29) and (30). □

When $(\theta+1)p$ approaches unity, the downlink channel would be very busy and little energy can be harvested at the mobile user. Thus, the uplink service time would be very large. As a result, the average uplink AoI goes to infinity and the uplink data rate goes to zero gradually, as observed in *Corollary* 4.

D. AVERAGE UPLINK AoI UNDER SAVE-AND-TRANSMIT POLICY

The save-and-transmit scheme was proposed in [26] and was proved to be able to approach the capacity of AWGN channels with energy harvesting. To be specific, an infinite long period of N blocks is divided into an energy saving period of $h(N) = o(N)$ blocks and an information transmission period of $N-h(N)$ blocks. During the energy saving period, all the harvested energy is stored in an infinitely large energy buffer. During the information transmission period, the transmitter performs transmission as if it has a constant power supply. As is proved, the probability that the transmitter is short of energy during the information transmission period is zero.

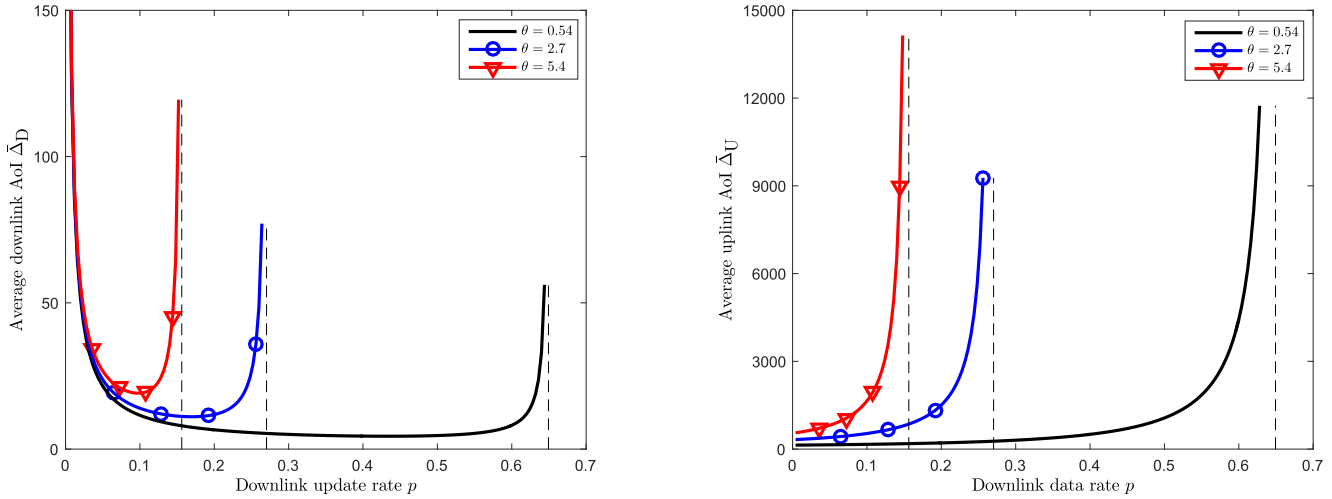

FIGURE 4. Average AoI of the two-way data exchange. (a) Average downlink AoI. (b) Average uplink AoI.

In our model, the save-and-transmit policy works as follows. The fog node generates data packets randomly and performs transmission as long as the data queue is non-empty; otherwise, it transfers energy to the mobile user. During the energy saving period, the mobile user saves all the harvested energy in an infinitely large buffer and keeps silent. In each block of the information transmission period, the mobile user generates a packet with probability q_{SV} and performs transmission at power $\beta P_{\mathrm{t}} T_{\mathrm{B}}$, as long as its data queue is non-empty. In particular, q_{SV} is chosen such that the expected energy consumption equals the expected energy harvesting. Since the best-effort policy can always exploit all the harvested energy, the data rate under the best-effort policy and the data rate under the save-and-transmit policy would be equal. Thus, q_{SV} can be determined based on (30). In particular, we have

$$q_{\mathrm{SV}} = \frac{(1-p)(1-p-\theta p)}{(\rho + e^{-\rho})(1+\frac{\theta}{\beta})(1-p+p^2+\theta p^2)}. \tag{31}$$

Following a similar arguments as that in [26], we can readily prove that the mobile user has sufficient energy for each transmitting block of the transmission period with probability one. Since $h(N) = o(N)$ is much smaller than N, the average uplink data rate of the whole period would be $q'_{\mathrm{sv}} = \frac{N-h(N)}{N} q_{\mathrm{SV}} = q_{\mathrm{SV}}$. Moreover, when the mobile user has sufficient energy for every necessary transmission, the corresponding average AoI can be obtained by replacing the data rate with q_{SV} in (16), which presents the average AoI under a constant power supply. We then have,

$$\overline{\Delta}_{\mathrm{SV}} = \frac{1}{q_{\mathrm{sv}}} + 1 + \frac{\theta}{\beta} + \frac{\theta(-2+4q_{\mathrm{sv}}+\frac{3\theta q_{\mathrm{sv}}}{\beta})}{2\beta(1-q_{\mathrm{sv}}-\frac{\theta q_{\mathrm{sv}}}{\beta})} + \frac{(1-q_{\mathrm{sv}}-\frac{\theta q_{\mathrm{sv}}}{\theta})(e^{\frac{\theta q_{\mathrm{sv}}}{\beta}}-1)}{q_{\mathrm{sv}}}. \tag{32}$$

For the save-and-transmit policy, although the long energy saving period can be removed by preparing some initial energy for the mobile user, it is still not very practical to implement since it requires very large energy buffers. Worse more, the mobile user would not wait for the downlink idle periods to transmit when save-and-transmit policy is used; and thus a full-duplex transceiver is needed at the fog node. However, the save-and-transmit policy often is the performance limit achieving scheme of a system and can serves as a benchmark scheme.

V. SIMULATION RESULTS

In this section, we investigate the AoI of the two-way data exchanging system via numerical and Monte Carlo results. The transmit power of the fog node is set to $P_{\mathrm{t}} = 0.01$ W for both transmitting information and transferring energy. The transmit power of the mobile user is also set to 0.01 W, i.e., $\beta = 1$. The system bandwidth is $\mathbb{W} = 100$ KHz, the noise spectrum density (including noise figure) is $\mathrm{N}_0 = 4 \times 10^{-7}$. The Rayleigh channel parameter is $\lambda = 3$, the block length is $T_{\mathrm{B}} = 10^{-3}$ s, and the energy transfer efficiency is $\eta = 0.5$. We set the distance between the two nodes to $d = 3$ m and pathloss exponent to $\alpha = 2$. On the length of each data packet, we consider the following three cases: $\ell = 0.5$ nats, $\ell = 2.5$ nats, and $\ell = 5$ nats. By using (3), parameter θ can be obtained as $\theta = 0.54$, $\theta = 2.7$, and $\theta = 5.4$, respectively. Note that for any given θ, the maximal downlink data rate enabling a stable queue at the fog node would be $p_{\max} = \frac{1}{1+\theta}$.

A. AVERAGE AoI

We present average downlink AoI $\overline{\Delta}_{\mathrm{D}}$ (c.f. (16)) in blocks in Fig. 4(a). We observe that $\overline{\Delta}_{\mathrm{D}}$ is a convex function of downlink data rate p. Thus, the minimum of $\overline{\Delta}_{\mathrm{D}}$ is obtained when p is neither too small nor too large. We also observe that when downlink data rate p approaches either zero or the maximal data rate $p_{\max}$ (shown by the dashed line), the average

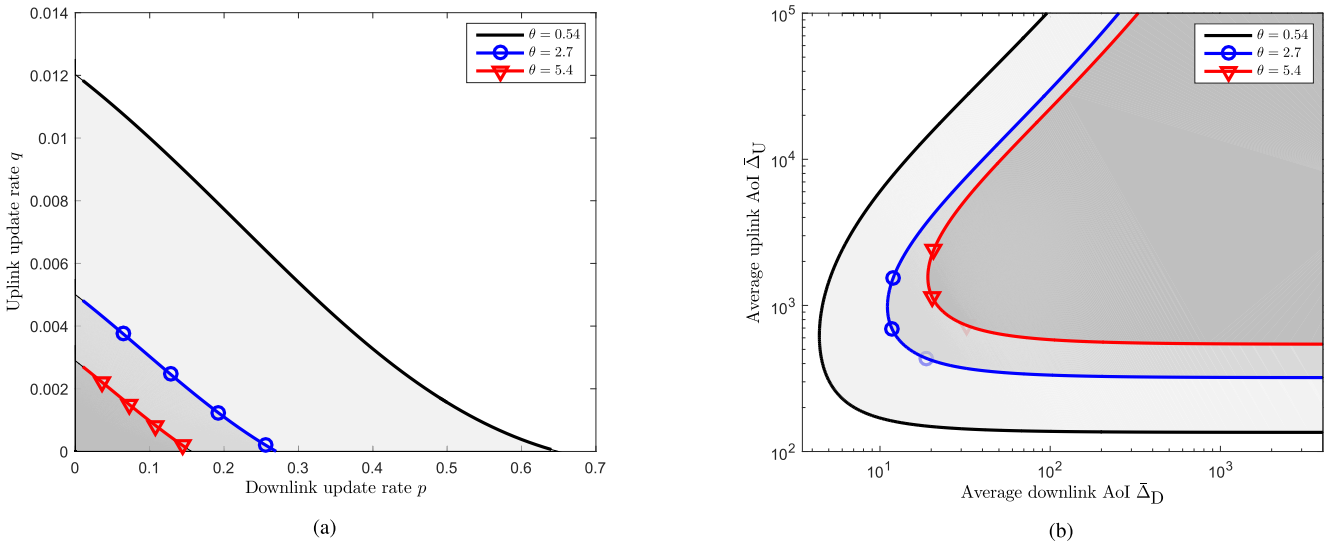

FIGURE 5. Downlink–uplink tradeoff. (a) Uplink data rate q. (b) Tradeoff between downlink and uplink AoI.

downlink AoI increases quickly, which is consistent with *Corollary* 1 and *Corollary* 2. Nevertheless, if we can choose a proper data rate, the average downlink AoI could be reasonably small. From Fig. 4(a), we also observe that average downlink AoI is increasing with θ while the maximal data rate $p_{\max}$ is decreasing with θ. This is because θ is the ratio between the packet length ℓ and the throughput of a block, i.e., $\theta = \frac{\ell}{\mathbb{E}(b)}$ (cf. (1), (3)). When θ is increased, both the service time and the waiting time of a packet would be larger, leading to larger average downlink AoI.

Fig. 4(b) depicts the average uplink AoI (cf. (29)). In general, the average uplink AoI is much larger than the average downlink AoI, especially when downlink data rate p is large. On one hand, if p is very small, the fog node would transfer energy to the mobile user for most of the time. In this case, the mobile user seldom needs to wait for harvesting energy so that uplink system time is determined only by the actual service time S. As p approaches zero, therefore, the average uplink AoI would converge to some constant, as shown in *Corollary* 3. On the other hand, as p approaches maximal data rate $p_{\max}$, the average uplink AoI goes to infinity, which is consistent with *Corollary* 4.

B. TWO-WAY DATA EXCHANGE TRADEOFF

We plot how uplink data rate q (cf. (30)) varies when downlink data p is changed in Fig. 5(a). We observe that q decreases approximately linearly when p is increased. In particular, q reduces to zero as p approaches $p_{\max}$. Moreover, for each given θ, the area under the curve can be regarded as the *achievable region* of data rate pair (p, q). That is, each point in the area under the curve is achievable while the points above the curve is not. Since the power supply at the fog node is the only energy source of the system, downlink data rate and uplink data rate cannot be optimized at the same time. Thus, the curves in Fig. 5(a) can also be regarded as best-achievable tradeoff between downlink data rate and uplink data rate. To see this clearly, one may use a weighted-sum

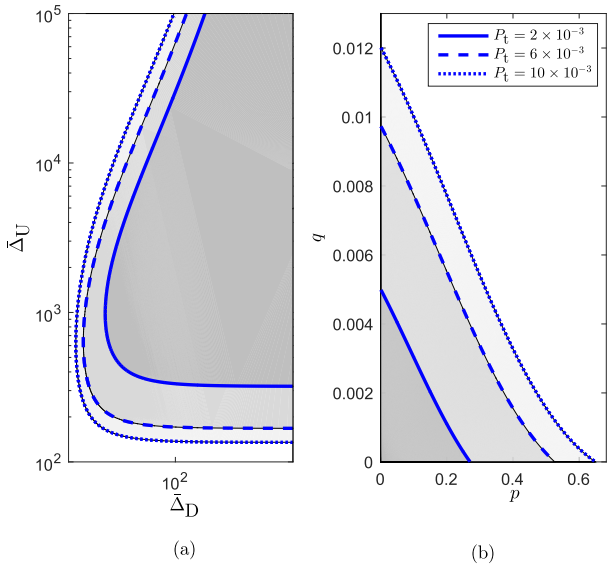

FIGURE 6. Average uplink AoI and uplink data rate tradeoff versus transmit power. (a) AoI tradeoff. (b) Data rate tradeoff.

characterization of system AoI. That is, a data rate pair (p, q) is said to be optimal if it maximizes the corresponding weighted sum $wp + (1 - w)q$, where $0 \leq w \leq 1$ is a constant showing the priority of downlink transmission and uplink transmission. Intuitively, the solution to this optimization can be obtained by searching the tangent point between line $wp + (1 - w)q = c$ and the curves in Fig. 5(a).

Fig. 5(b) presents the tradeoff between average downlink AoI and average uplink AoI, which are obtained according to *Theorem* 1 and *Theorem* 2, respectively. We observe that the average uplink AoI is not a convex function of average downlink AoI. This is because the average downlink AoI is not a monotonic function of downlink data rate p, as shown in Fig. 4(a). For a given θ, the corresponding AoI curve can also be regarded as the boundary of the achievable region for average AoI pair $(\bar{\Delta}_{\mathrm{D}}, \bar{\Delta}_{\mathrm{U}})$. Moreover, the points on

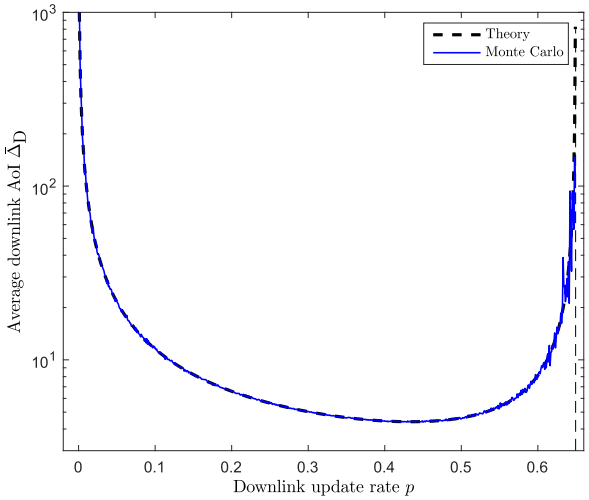

(a)

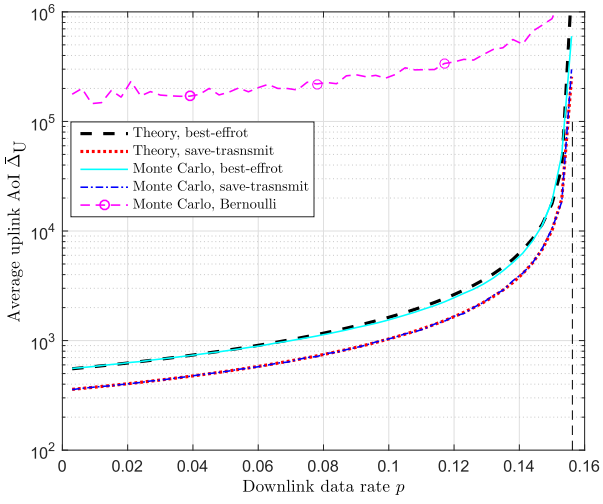

(b)

FIGURE 7. Theoretical and Monte Carlo results. (a) Average downlink AoI. (b) Average uplink AoI.

the boundary are the solutions to the average weight-sum AoI minimization problem of the two-way data exchanging system, and thus specifies the optimal system performance in terms of timeliness.

We further investigate how transmit power P_t affects the tradeoff of average downlink/uplink AoI and downlink/uplink data rate in Fig. 6. We observe that for both directions, average AoIs are decreasing with P_t and data rates are increasing with P_t. Moreover, the marginal gain of increasing P_t decreases as P_t becomes larger and larger.

C. MONTE CARLO SIMULATIONS AND SAVE-AND-TRANSMIT POLICY

In this subsection, we verify our results with Monte Carlo simulation. Packet length is set to $\ell = 5$ nats and simulation time is set to $T_{mc} = 10^4$ s, i.e., 10^7 blocks of transmissions. As shown in Fig. 7(a), our theoretical results (cf. (16)) on the average downlink AoI coincide with the corresponding Monte Carlo results perfectly. Fig. 7(b) presents the average uplink AoI of both the best-effort policy and the save-and-forward policy. First, we observe that for the best-effort policy, the theoretical result (cf. (29)) coincide with the Monte Carlo result very well except slight deviation when p is large. This is due to the assumption that the harvested energy in each block can support one block of transmission at most (cf. *Remark* 2). Since the channel condition is very good and the mobile user can harvest a large amount of energy in the Monte Carlo simulation, the remaining energy e_r could be the accumulation of the energy harvested in several blocks and does not follow exponential distribution. Nevertheless, if the Rayleigh parameter λ is larger, energy transfer efficiency η is smaller, and the distance between the two node is larger, the deviation decreases. Second, we observe that the average AoI of the save-and-transmit policy is smaller. This is because for the best-effort policy, an uplink packet is generated immediately after the completion of previous one, no matter the mobile user has enough energy or not, which increases AoI slightly. Although the best-effort policy experiences slightly larger AoI, it is practical and easy to implement. Thus, the best-effort policy is a good choice for real implementations. Third, we observe that when packet are generated in each block with a Bernoulli process (cf. the purple circled curve), the average uplink AoI is much larger than that when packets are generated by the best-effort policy. In fact, the best-effort reduces AoI significantly by exploring the queueing information, i.e., no packet is generated unless the current one is completed. The Bernoulli packet generation process, however, would lead to large average AoI due to extra waiting time in the queueing process.

VI. CONCLUSION

In this paper, we have studied the timeliness of a two-way data exchanging FC system with a unique power supply at the fog node. We obtained average AoI for the data exchange in both directions and presented their asymptotic behaviors. Based on these results, we have also determined the achievable region of average downlink AoI and average uplink AoI, as well as the achievable region of downlink data rate and uplink data rate. It is clear that both the downlink performance and the uplink performance are constrained by the limited transmit power of the fog node. Moreover, the uplink performance is also effected by downlink data rate p. That is, the average uplink AoI would be smaller and the average uplink data rate would be larger if p is decreased. Since the downlink performance and the uplink performance cannot be optimized at the same time, one needs to find the tradeoff between them under some criteria, e.g., weighted-min/max criteria, as discussed in Subsection V-B and Fig. 5. Thus, the obtained results have fully characterized the data exchanging capability of the FC system.

Different from traditional capacity analysis where the data queue of users are saturated, we have considered the timeliness of a FC system with bursty traffics. In this regard,

we have obtained the stability region of the system in terms of downlink data rate and uplink data rate. We also would like to mention that the unilaterally powered FC system in this paper is a smallest cooperative system with bursty traffics. To be specific, since the fog node undergos idle periods frequently, a cooperation between the fog node and the mobile user can be established by transferring energy during idle periods. This cooperation is important in that it makes the batteryless uplink communication possible while the performance of downlink communication is unaffected. Moreover, this kind of cooperation can readily be generalized to other networks with more than one node and can be realized either by transferring energy or transmitting cooperative information.

APPENDIX

A. PROOF OF PROPOSITION 1

Proof: For the case $A_k = 0$, we have

$$\begin{aligned} p_0^{\mathrm{a}} &= \sum_{m=1}^{\infty} \Pr\{S_{\mathrm{D}k} = m\} \Pr\{A_k = 0 | S_{\mathrm{D}k} = m\} \\ &= (1-p)e^{-\theta p}, \end{aligned}$$

where $\Pr\{S_{\mathrm{D}k} = m\} = p_m^{\mathrm{s}}$ is given by (2).

For $j \geq 1$, we have

$$\begin{aligned} p_j^{\mathrm{a}} &= \sum_{m=j}^{\infty} p_m^{\mathrm{s}} \binom{m}{j} (1-p)^{m-j} p^j \\ &= \sum_{m=j}^{\infty} \frac{\theta^{m-1}}{(m-1)!} e^{-\theta} \frac{m!}{j!(m-j)!} (1-p)^{m-j} p^j \\ &= e^{-\theta} \frac{p^j}{j!} \theta^{j-1} \sum_{m=0}^{\infty} (m+j) \frac{(\theta(1-p))^m}{m!} \\ &= (1-p)e^{-\theta p} \frac{(\theta p)^j}{j!} + p e^{-\theta p} \frac{(\theta p)^{j-1}}{(j-1)!}. \end{aligned}$$

Thus, the PGF of A_k is

$$\begin{aligned} G_{\mathrm{A}}(z) &= \mathbb{E}(z^{A_k}) = \sum_{j=0}^{\infty} p_j^{\mathrm{a}} z^j \\ &= (1-p)e^{-\theta p} \sum_{j=0}^{\infty} \frac{(\theta p z)^j}{j!} + p e^{-\theta p} z \sum_{j=1}^{\infty} \frac{(\theta p z)^{j-1}}{(j-1)!} \\ &= (1-p+pz)e^{\theta p(z-1)}. \end{aligned}$$

□

B. PROOF OF PROPOSITION 3

Proof: Under the FCFS serving policy, the queue length at a departure epoch equals the number of arriving packets during the system time of the leaving packet. Thus, for $j = 0, 1, 2, \cdots$, we have

$$\Pr\{L_{\mathrm{d}}^+(k) = j\} = \sum_{i=j}^{\infty} \Pr\{T_{\mathrm{D}k} = i\} \binom{i}{j} p^j (1-p)^{i-j}.$$

The PGF of $G_{L_{\mathrm{d}}^+}(s) = \mathbb{E}(s^{L_{\mathrm{d}}^+})$ can then be expressed as

$$\begin{aligned} G_{L_{\mathrm{d}}^+}(s) &= \sum_{j=0}^{\infty} s^j \sum_{i=j}^{\infty} \Pr\{T_{\mathrm{D}k} = i\} \binom{i}{j} p^j (1-p)^{i-j} \\ &= \sum_{i=0}^{\infty} \Pr\{T_{\mathrm{D}k} = i\} \sum_{j=0}^{i} \binom{i}{j} (ps)^j (1-p)^{i-j} \\ &= \sum_{i=0}^{\infty} \Pr\{T_{\mathrm{D}k} = i\} (1-p+ps)^i \\ &= G_{T_{\mathrm{D}}}(1-p+ps). \end{aligned} \tag{A.33}$$

Combining (13) in Proposition 2, (A.33), and using substitution $z = 1-p+ps$, the proof of the proposition would be completed. □

C. PROOF OF THEOREM 1

Proof: According to Proposition 2, the queue is not stable and queue length would be infinitely large in the case of $p(\theta+1) \geq 1$. Thus, the average downlink AoI would also be infinitely large. Next, we consider the case of $p(\theta+1) < 1$.

From Fig. 2, it is clear that Q_0 is finite. Also note that the service time of the last packet is finite with probability one. Therefore, as time N goes to infinity, the average downlink AoI (cf. (8)) can be rewritten as

$$\begin{aligned} \overline{\Delta}_{\mathrm{D}} &= \lim_{N\to\infty} \frac{1}{N} \sum_{k=1}^{K-1} Q_k \\ &= \lim_{N\to\infty} \frac{K-1}{N} \frac{1}{K-1} \sum_{k=1}^{K-1} Q_k \\ &= p\mathbb{E}(Q_k), \end{aligned} \tag{A.34}$$

where $\lim_{N\to\infty} \frac{K-1}{N} = p$ is the arrival rate of data packets at the fog node.

Moreover, the average area of each Q_k is

$$\begin{aligned} \mathbb{E}(Q_k) &= \mathbb{E}\Big(\frac{1}{2} X_k(X_k+1) + X_k T_{\mathrm{D}k}\Big) \\ &= \frac{1}{2}\mathbb{E}(X_k) + \frac{1}{2}\mathbb{E}(X_k^2) + \mathbb{E}(X_k T_{\mathrm{D}k}). \end{aligned} \tag{A.35}$$

Since the arrival of packets follows Bernoulli distribution with parameter p, the inter-arrival time X_k follows Geometric distribution, i.e., $\Pr\{X_k = j\} = (1-p)^{j-1}p, j = 1, 2, \cdots$. Hence, the first and second moment of X_k are, respectively, given by

$$\mathbb{E}(X_k) = \frac{1}{p}, \quad \mathbb{E}(X_k^2) = \frac{2-p}{p^2}. \tag{A.36}$$

From Fig. 2, we know that downlink system time is $T_{\mathrm{D}k} = W_{\mathrm{D}k} + S_{\mathrm{D}k}$. In addition, the waiting time $W_{\mathrm{D}k}$ is zero if packet $k-1$ has already been served upon the k-th packet arrival, and equals to $T_{\mathrm{D}k-1} - X_k$ if packet $k-1$ is either under service or waiting. Thus, we have $W_{\mathrm{D}k} = \max(0, T_{\mathrm{D}k-1} - X_k)$ and know that X_k is correlated with W_k. In particular, we have

$$\mathbb{E}(X_k T_{\mathrm{D}k}) = \mathbb{E}(X_k)\mathbb{E}(S_{\mathrm{D}k}) + \mathbb{E}(X_k W_{\mathrm{D}k}) \tag{A.37}$$

Before we proceed, one useful lemma is presented as follows [23].

Lemma 2: Suppose Y is a random variable of non-negative integers, then we have

$$\mathbb{E}(Y)=\sum_{k=0}^{\infty}\Pr\{Y>k\},\quad \sum_{k=0}^{\infty}z^k\Pr\{Y>k\}=\frac{1-G_{\rm Y}(z)}{1-z},$$

where $G_{\rm Y}(z)$ is the PGF of Y.

To calculate $\mathbb{E}(X_kT_{{\rm D}k})$, we define $H_{\rm D}(z)$ as

$$H_{\rm D}(z)=\sum_{i=1}^{\infty}\Pr\{X_k=i\}z^i\sum_{j=0}^{\infty}\Pr\{T_{{\rm D}k-1}>i+j\}.$$

By performing a detailed analysis on $H_{\rm D}(z)$, we have

$$\begin{aligned}H_{\rm D}(z)&=\sum_{i=1}^{\infty}z^i\Pr\{X_k=i\}\sum_{j=i}^{\infty}\Pr\{T_{{\rm D}k-1}>j\}\\&=\sum_{j=1}^{\infty}\sum_{i=1}^{j}\Pr\{X_k=i\}\Pr\{T_{{\rm D}k-1}>j\}z^i\\&=\sum_{j=1}^{\infty}\Pr\{T_{{\rm D}k-1}>j\}pz\frac{1-(1-p)^jz^j}{1-(1-p)z}\\&=\frac{pz}{1-(1-p)z}\left(\mathbb{E}(T_{{\rm D}k-1})-\frac{1-G_{\rm T_D}((1-p)z)}{1-(1-p)z}\right),\end{aligned}$$

where the last equation follows Lemma 2. In addition, $\mathbb{E}(T_{{\rm D}k-1})$ and $G_{\rm T_D}(z)$ are given by (14) and (15), respectively.

We further note that

$$\begin{aligned}&\mathbb{E}(X_kW_{{\rm D}k})\\&=\mathbb{E}\left(X_k\mathbb{E}(\max(0,T_{{\rm D}k-1}-X_k))\right)\\&=\sum_{i=1}^{\infty}i\Pr\{X_k=i\}\sum_{j=0}^{\infty}\Pr\{\max(0,T_{{\rm D}k-1}-i)>j\}\\&=\sum_{i=1}^{\infty}i\Pr\{X_k=i\}\sum_{j=0}^{\infty}\Pr\{T_{{\rm D}k-1}>i+j\}\\&=\lim_{z\to1^-}(H_{\rm D}(z))'\\&=\lim_{z\to1^-}\frac{p\mathbb{E}(T_{{\rm D}k-1})}{(1-(1-p)z)^2}-\frac{p(1+(1-p)z)}{(1-(1-p)z)^3}\\&\quad\cdot(1-G_{\rm T_D}((1-p)z))+\frac{p(1-p)z}{(1-(1-p)z)^2}G'_{\rm T_D}((1-p)z)\\&=\frac{(-2+4p+3\theta p)\theta}{2p(1-p-\theta p)}+\frac{(1-p-\theta p)(e^{\theta p}-1)}{p^2},\end{aligned}\tag{A.38}$$

where $G_{\rm T_D}(1-p)=1-p-\theta p$ and $G'_{\rm T_D}(1-p)=\frac{(1-p-\theta p)(p-1+e^{\theta p})}{p(1-p)}$ are derived from (15).

Combining the results in (5) and (A.34)–(A.38), we have

$$\begin{aligned}\overline{\Delta}_{\rm D}&=p\Big(\frac{1}{2}\mathbb{E}(X_k)+\frac{1}{2}\mathbb{E}(X_k^2)+\mathbb{E}(X_k)\mathbb{E}(S_{{\rm D}k})+\mathbb{E}(X_kW_{{\rm D}k})\Big)\\&=\frac{1}{p}+1+\theta+\frac{(-2+4p+3\theta p)\theta}{2(1-p-\theta p)}+\frac{(1-p-\theta p)(e^{\theta p}-1)}{p}.\end{aligned}$$

This completes the proof of *Theorem* 1. □

D. PROOF OF PROPOSITION 4

Proof: Since the actual time to perform a block of uplink transmission is $s=\max\{1,\tau_{\rm H}\}$, we have $\Pr\{s=0\}=0$ and $\Pr\{s=1\}=\Pr\{\tau_{\rm H}=0\}+\Pr\{\tau_{\rm H}=1\}$.

Based on (19), we have $\mathbb{E}(\tau_{\rm H})=\rho$ and $\mathbb{E}(\tau_{\rm H}^2)=\rho^2+\rho$. Thus, we have $\mathbb{E}(s)=\mathbb{E}(\tau_{\rm H})+\Pr\{\tau_{\rm H}=0\}=\rho+e^{-\rho}$ and $\mathbb{E}(s^2)=\mathbb{E}(\tau_{\rm H}^2)+\Pr\{\tau_{\rm H}=0\}=\rho^2+\rho+e^{-\rho}$. By using (21), we then have

$$\mathbb{E}(S_{\rm U})=\mathbb{E}(S_{\rm Tx})\mathbb{E}(s)=(\rho+e^{-\rho})\left(1+\frac{\theta}{\beta}\right),$$

and

$$\begin{aligned}\mathbb{E}(S_{\rm U}^2)&=\mathbb{E}\left(\sum_{i=1}^{S_{\rm Tx}}s_i^2+\sum_{i=1}^{S_{\rm Tx}}\sum_{j\neq i}^{S_{\rm Tx}}s_is_j\right)\\&=\mathbb{E}(S_{\rm Tx})\mathbb{E}(s^2)+\mathbb{E}(S_{\rm Tx}^2-S_{\rm Tx})\mathbb{E}^2(s)\\&=(\rho+e^{-\rho})^2(\frac{\theta^2}{\beta^2}+\frac{2\theta}{\beta})+(\rho^2+\rho+e^{-\rho})(1+\frac{\theta}{\beta}).\end{aligned}$$

This completes the proof of the proposition. □

E. PROOF OF PROPOSITION 5

Proof: Note that the length of a busy period is independent from the order of service. Thus, we assume the Last Come First Service (LCFS) discipline in this proof. In this case, busy period $B_{\rm D}$ is the concatenation of service time S of the first data packet of the busy period, and busy periods $B_{{\rm D}l}^{(i)}$ which are generated by the packets arriving during the service time of the first packet. Denote the number of packets arriving during the service time of the first packet by κ, we have

$$B_{\rm D}=S+B_{\rm D}^{(1)}+B_{\rm D}^{(2)}+\cdots+B_{\rm D}^{(\kappa)}.$$

Given $S=j$ and $\kappa=m$, we have

$$\begin{aligned}\mathbb{E}\big(z^{B_{\rm D}}|S=j,\kappa=m\big)&=\mathbb{E}\big(z^{j+B_{\rm D}^{(1)}+B_{\rm D}^{(2)}+\cdots+B_{\rm D}^{(m)}}\big)\\&=z^j\big(G_{B_{\rm D}}(z)\big)^m.\end{aligned}$$

According to the law of total probability, we have

$$\begin{aligned}G_{B_{\rm D}}(z)&\sum_{j=1}^{\infty}\sum_{m=0}^{j}\mathbb{E}\big(z^{B_{\rm D}}|S=j,\kappa=m\big)\\&\cdot\Pr\{S=j\}\Pr\{\kappa=m|S=j\}\\&=\sum_{j=1}^{\infty}\sum_{m=0}^{j}\mathbb{E}\big(z^{B_{\rm D}}|S=j,\kappa=m\big)\binom{j}{m}p^m(1-p)^{j-m}p_j^{\rm s}\\&=\sum_{j=1}^{\infty}p_j^{\rm s}z^j\sum_{m=0}^{j}\binom{j}{m}\big(pG_{B_{\rm D}}(z)\big)^m(1-p)^{j-m}\\&=G_{\rm S}\big(z(1-p+pG_{B_{\rm D}}(z))\big),\end{aligned}\tag{A.39}$$

where $G_{\rm S}(z)$ is the PGF of service time S (cf. (4)).

Taking derivative on both sides of (A.39), let $z\to1^-$, and solving equation $\mathbb{E}(B_{\rm D})=G'_{B_{\rm D}}(1^-)$, we have

$$\mathbb{E}(B_{\rm D})=\frac{1+\theta}{1-p-\theta p}.$$

Taking the second-order derivative on both sides of (A.39), letting $z \to 1^-$, and solving $G''_{B_D}(1^-)$, we have

$$G''_{B_D}(1^-) = \frac{2(1+\theta)^2 p}{(1-p-\theta p)^2} + \frac{\theta^2 + 2\theta^2}{(1-p-\theta p)^3}.$$

By using $\mathbb{E}(B_D^2) = G''_{B_D}(1^-) + G'_{B_D}(1^-)$, we have

$$\mathbb{E}(B_D^2) = \frac{(1+\theta)^2(1-p^2-\theta p^2)+\theta}{(1-p-\theta p)^3}.$$

This completes the proof of the proposition. □

F. PROOF OF THEOREM 2

Proof: According to Proposition 2, the queue length at the fog node would be infinitely large if $p(\theta+1) \geq 1$. That is, the fog node will be always in the busy period and no energy can be transferred to the mobile user. In this case, the average uplink AoI would be infinitely large and the uplink data rate would be zero. Next, we consider the case of $p(\theta+1) < 1$.

According to the definition of uplink data rate (10), we have

$$\begin{aligned} q &= \lim_{N\to\infty} \frac{K}{N} = \frac{1}{\mathbb{E}(T_U)} \\ &= \frac{(1-p)(1-p-\theta p)}{(\rho + e^{-\rho})(1+\frac{\theta}{\beta})(1-p+p^2+\theta p^2)}, \end{aligned} \tag{A.40}$$

where $\mathbb{E}(T_U)$ is calculated based on (23)–(28).

In the definition of $\overline{\Delta}_U$ (cf. (9)), we note that Q_0 is finite and T_{Uk} is finite in probability. Thus, the average uplink AoI can be rewritten as

$$\overline{\Delta}_U = \lim_{N\to\infty} \frac{1}{N} \sum_{k=1}^{K-1} Q_k \tag{A.41}$$

$$= \lim_{N\to\infty} \frac{K-1}{N} \frac{1}{K-1} \sum_{k=1}^{K-1} Q_k \tag{A.42}$$

$$= q\mathbb{E}(Q_k). \tag{A.43}$$

Note that the average of area Q_k is given by

$$\begin{aligned} \mathbb{E}(Q_k) &= \mathbb{E}\Big(T_{Uk}T_{Uk+1} + \frac{1}{2}T_{Uk}\big(T_{Uk}+1\big)\Big) \\ &= \mathbb{E}^2\big(T_U\big) + \frac{1}{2}\mathbb{E}\big(T_U^2\big) + \frac{1}{2}\mathbb{E}\big(T_U\big). \end{aligned} \tag{A.44}$$

By combining the results in *Proposition* 6 and equations (A.40)–(A.44), the average uplink AoI can be rewritten as

$$\begin{aligned} \overline{\Delta}_U &= \mathbb{E}\big(T_U\big) + \frac{1}{2} + \frac{1}{2}\frac{\mathbb{E}\big(T_U^2\big)}{\mathbb{E}(T_U)} \\ &= \frac{p(1+\theta)^2 - p^3(2-p)(1+\theta)^3 + \theta p(1-p)}{2(1-p)(1-p-\theta p)^2(1-p+p^2+\theta p^2)} \\ &\quad + \left(\frac{\rho^2+\rho+e^{-\rho}}{\rho+e^{-\rho}} + (\rho+e^{-\rho})\frac{\frac{3\theta^2}{\beta^2}+\frac{6\theta}{\beta}+2}{1+\frac{\theta}{\beta}}\right) \\ &\quad \cdot \frac{1-p+p^2+\theta p^2}{2(1-p)(1-p-\theta p)} + \frac{1}{2}. \end{aligned}$$

Thus, the proof of *Theorem* 2 is completed. □

ACKNOWLEDGMENT

This paper was presented in part at the 2018 IEEE International Conference on Computer Communications, Age of Information Workshop (*IEEE INFOCOM'18 AoI Wksh*).

REFERENCES

[1] J. Zheng, D. Simplot-Ryl, C. Bisdikian, and H. T. Mouftah, "The Internet of Things," *IEEE Commun. Mag.*, vol. 49, no. 11, pp. 30–31, Nov. 2011.
[2] Cisco, "Cisco visual networking index: Global mobile data traffic forecast update, 2015–2020," Cisco, San Jose, CA, USA, White Paper, Feb. 2016.
[3] A. U. R. Khan, M. Othman, S. A. Madani, and S. U. Khan, "A survey of mobile cloud computing application models," *IEEE Commun. Surveys Tuts.*, vol. 16, no. 1, pp. 393–413, 1st Quart., 2014.
[4] W. Zhang, Y. Wen, K. Guan, D. Kilper, H. Luo, and D. O. Wu, "Energy-optimal mobile cloud computing under stochastic wireless channel," *IEEE Trans. Wireless Commun.*, vol. 12, no. 9, pp. 4569–4581, Sep. 2013.
[5] S. Wang, X. Zhang, Y. Zhang, L. Wang, J. Yang, and W. Wang, "A survey on mobile edge networks: Convergence of computing, caching and communications," *IEEE Access*, vol. 5, pp. 6757–6779, 2017.
[6] Y. C. Hu, M. Patel, D. Sabella, N. Sprecher, and V. Young, "Mobile edge computing: A key technology towards 5G," Eur. Telecommun. Standards Inst., Sophia Antipolis, White Paper 11, France, 2015.
[7] F. Bonomi, R. Milito, J. Zhu, and S. Addepalli, "Fog computing and its role in the Internet of Things," in *Proc. 1st Ed. Workshop Mobile Cloud Comput. (MCC)*, Aug. 2012, pp. 13–16.
[8] C. Zhang, P. Fan, K. Xiong, and P. Fan, "Optimal power allocation with delay constraint for signal transmission from a moving train to base stations in high-speed railway scenarios," *IEEE Trans. Veh. Technol.*, vol. 64, no. 12, pp. 5775–5788, Dec. 2015.
[9] S. Bi and Y. J. Zhang, "Computation rate maximization for wireless powered mobile-edge computing with binary computation offloading," *IEEE Trans. Wireless Commun.*, vol. 17, no. 6, pp. 4177–4190, Jun. 2018.
[10] K. Xiong, C. Chen, G. Qu, P. Fan, and K. B. Letaief, "Group cooperation with optimal resource allocation in wireless powered communication networks," *IEEE Trans. Wireless Commun.*, vol. 16, no. 6, pp. 3840–3853, Jun. 2017.
[11] F. Wang, "Computation rate maximization for wireless powered mobile edge computing," in *Proc. 23rd Asia–Pacific Conf. Commun. (APCC)*, Perth, WA, Australia, Dec. 2017, pp. 1–6.
[12] X. Hu, K.-K. Wong, and K. Yang, "Wireless powered cooperation-assisted mobile edge computing," *IEEE Trans. Wireless Commun.*, vol. 17, no. 4, pp. 2375–2388, Apr. 2018.
[13] S. Mao, S. Leng, K. Yang, X. Huang, and Q. Zhao, "Fair energy-efficient scheduling in wireless powered full-duplex mobile-edge computing systems," in *Proc. IEEE Global Commun. Conf. (GLOBECOM)*, Singapore, Dec. 2017, pp. 1–6.
[14] S. Mao, S. Leng, K. Yang, Q. Zhao, and M. Liu, "Energy efficiency and delay tradeoff in multi-user wireless powered mobile-edge computing systems," in *Proc. IEEE Global Commun. Conf. (GLOBECOM)*, Singapore, Dec. 2017, pp. 1–6.
[15] S. Kaul, R. Yates, and M. Gruteser, "Real-time status: How often should one update?" in *Proc. IEEE INFOCOM*, Orlando, FL, USA, Mar. 2012, pp. 2731–2735.
[16] A. M. Bedewy, Y. Sun, and N. B. Shroff, "Optimizing data freshness, throughput, and delay in multi-server information-update systems," in *Proc. IEEE Int. Symp. Inf. Theory (ISIT)*, Barcelona, Spain, Jul. 2016, pp. 2569–2573.
[17] Y. Sun, E. Uysal-Biyikoglu, R. D. Yates, C. E. Koksal, and N. B. Shroff, "Update or wait: How to keep your data fresh," *IEEE Trans. Inf. Theory*, vol. 63, no. 11, pp. 7492–7508, Nov. 2017.
[18] M. Costa, M. Codreanu, and A. Ephremides, "On the age of information in status update systems with packet management," *IEEE Trans. Inf. Theory*, vol. 62, no. 4, pp. 1897–1910, Apr. 2016.
[19] C. Kam, S. Kompella, G. D. Nguyen, J. E. Wieselthier, and A. Ephremides, "Controlling the age of information: Buffer size, deadline, and packet replacement," in *Proc. IEEE Mil. Commun. Conf. (MILCOM)*, Baltimore, MD, USA, Nov. 2016, pp. 301–306.
[20] J. Walk, J. Weber, C. Soell, R. Weigel, G. Fischer, and T. Ussmueller, "Remote powered medical implants for telemonitoring," *Proc. IEEE*, vol. 102, no. 11, pp. 1811–1832, Nov. 2014.

[21] A. Yakovlev, S. Kim, and A. Poon, "Implantable biomedical devices: Wireless powering and communication," *IEEE Commun. Mag.*, vol. 50, no. 4, pp. 152–159, Apr. 2012.
[22] Y. Dong, Z. Chen, and P. Fan, "Uplink age of information of unilaterally powered two-way data exchanging systems," in *Proc. IEEE Conf. Comput. Commun. Workshops (INFOCOM)*, Honolulu, HI, USA, Apr. 2018, pp. 559–564.
[23] Y. Dong and P. Fan, "Queueing analysis for block fading Rayleigh channels in the low SNR regime," in *Proc. Int. Conf. Wireless Commun. Signal Process. (WCSP)*, Hangzhou, China, Oct. 2013, pp. 1–6.
[24] P. Brémaud, *Lyapunov Functions and Martingales*. New York, NY, USA: Springer, 1999, pp. 167–193.
[25] A. E. Taylor, "L'Hôpital's rule," *Amer. Math. Monthly*, vol. 59, no. 1, pp. 20–24, Jan. 1952.
[26] O. Ozel and S. Ulukus, "Achieving AWGN capacity under stochastic energy harvesting," *IEEE Trans. Inf. Theory*, vol. 58, no. 10, pp. 6471–6483, Oct. 2012.

YUNQUAN DONG (M'15) received the M.S. degree in communication and information systems from the Beijing University of Posts and Telecommunications, Beijing, China, in 2008, and the Ph.D. degree in communication and information engineering from Tsinghua University, Beijing, in 2014. He was a BK Assistant Professor with the Department of Electrical and Computer Engineering, Seoul National University, Seoul, South Korea. He is currently a Professor with the School of Electronic and Information Engineering, Nanjing University of Information Science and Technology, Nanjing, China.

His research interests include performance evaluation and performance optimization in wireless networks, e.g., energy harvesting systems and vehicular networks. He was selected as an Exemplary Reviewer of IEEE Wireless Communications Letters, in 2017. He was a recipient of the Outstanding Graduate Award of Beijing with Honors, in 2014. He received the Best Paper Award from the IEEE ICCT, in 2011, the National Scholarship for Postgraduates from the China's Ministry of Education, in 2013, and the Young Star of Information Theory Award from the China's Information Theory Society, in 2014.

ZHENGCHUAN CHEN (M'16) received the B.S. degree from Nankai University, China, in 2010, and the Ph.D. degree from Tsinghua University, China, in 2015. He visited The Chinese University of Hong Kong, in 2012, and visited the University of Florida, USA, in 2013. From 2015 to 2017, he was a Postdoctoral Fellow with the Information Systems Technology and Design Pillar, Singapore University of Technology and Design. He is currently an Assistant Professor with the School of Microelectronics and Communication Engineering, Chongqing University, China. His main research interests include the Internet of Things, energy harvesting, and network information theory.

Dr. Chen was selected as an Exemplary Reviewer of the IEEE Transactions on Communications, in 2015. He co-received the Best Paper Award from the International Workshop on High Mobility Wireless Communications, in 2013. He has served for several IEEE conferences, e.g., the IEEE Globecom, as a Technical Program Committee Member.

PINGYI FAN (M'03–SM'09) received the B.S. degree from the Department of Mathematics, Hebei University, in 1985, the M.S. degree from Nankai University, in 1990, and the Ph.D. degree from the Department of Electronic Engineering, Tsinghua University, Beijing, China, in 1994. From 1997 to 1998, he visited The Hong Kong University of Science and Technology, as a Research Associate. From 1998 to 1999, he visited the University of Delaware, USA, as a Research Fellow. In 2005, he visited NICT, Japan, as a Visiting Professor. From 2005 to 2011, he visited The Hong Kong University of Science and Technology for many times. In 2011, he was a Visiting Professor with the Institute of Network Coding, The Chinese University of Hong Kong. He is currently a Professor with the Department of Electrical Engineering, Tsinghua University.

His main research interests include B4G technology in wireless communications, such as multi-in multi-out and OFDMA, network coding, network information theory, and cross-layer design. Dr. Fan is a Senior Member of the IEEE and an Oversea Member of the IEICE. He has received some academic awards, including the IEEE WCNC 2008 Best Paper Award, the ACM IWCMC 2010 Best Paper Award, and the IEEE ComSoc Excellent Editor Award of the IEEE Transactions on Wireless Communications, in 2009. He has attended to organize many international conferences, including the TPC Co-Chair of the IEEE International Conference on Wireless Communications, Networking and Information Security (WCNIS 2010) and a TPC Member of the IEEE ICC, Globecom, WCNC, and VTC. He has served as an Editor for the IEEE Transactions on Wireless Communications, the *Inderscience International Journal of Ad Hoc and Ubiquitous Computing*, and the *Wiley Journal of Wireless Communication and Mobile Computing*. He is also a Reviewer for more than 24 international journals, including 12 IEEE journals and eight EURASIP journals.